An image processing approach to fast, efficient proximity correction for electron beam lithography

D. G. L. Chow, J. F. McDonald, D. C. King, W. Smith, K. Molnar, and A. J. Steckl

Center for Integrated Electronics, Rensselaer Polytechnic Institute, Troy, New York 12181

(Received 3 June 1983; accepted 12 September 1983)

A limitation on the quality of electron beam lithography is the proximity effect. This produces exposure of the resist at locations remote from the point of incidence of the electron beam. One of the techniques used to mitigate this problem is to precompensate the applied beam dose. Traditional approaches to this problem have required extensive calculations which occasionally fail to produce satisfactory results. However, the proximity correction problem is quite similar to the edge enhancement problem which arises in pattern recognition. Furthermore, the issue of data base compaction for the precompensated lithography is quite similar to bandwidth compression in image transmission. In this paper, we examine the application of image processing methods to the proximity correction problem. We find that, while the match between these disciplines is not perfect, the idea appears quite promising.

PACS numbers: 85.40. — e

I. INTRODUCTION

Electron beam lithography suffers from the proximity effect[1] wherein electron scattering from the resist and the substrate produces some exposure at locations remote from the point of incidence of the electron beam. The problem becomes more severe as the dimensions of the lithographic features approach 1 μm or less. The effect becomes most troublesome when features of somewhat different dimensions lie closely packed in the desired artwork. As a result of intraproximity effects, some pattern shapes will be larger or smaller than desired, some will be separated by insufficiently wide gaps, and corners will become rounded. In some cases, some features are lost altogether. Obviously, this seriously degrades the quality of the lithography in the near-micron and submicron region.

Various physical methods for reducing the scattered electrons have been considered. An excellent critical review of the area by Hawryluk[2] discusses many of these. It has also been suggested that ion beams can exhibit extremely low proximity effects.[3] Nevertheless, it is still of interest to improve electron beam lithography where possible.

Two approaches have emerged to correct for the proximity effect. One involves adjusting the pattern dimensions[4] and the other involves precompensation of the applied beam dose.[5] Algorithms for determining the optimum dimensions or adjusting the dose values require extensive calculations which occasionally fail to produce satisfactory artwork because of compromises required by each method. Furthermore, neither of these approaches fully exploits the advantages provided by special purpose computing hardware (such as the Floating Point Systems model 164 attached array processor) which are commercially available.

Of these two traditional approaches to proximity correction, dose precompensation is the most widely used and understood. The usual approach is to arbitrarily subdivide a given region into subregions in which the applied dose is made constant.[6] Next, the net effective dose in the resist is computed at a variety of arbitrarily selected sample points in terms of the applied doses. A set of sparse linear equations is obtained which are solved for the applied doses given desired effective doses in the resist. In this method, direct control is obtained over the size of the resulting data base which depends on the partitioning method used to select the constant dose subregions. However, the accuracy of the result is weakened by the arbitrary way in which the subregions and effective dose sample points are chosen. To keep the complexity of the computation manageable, compromises are inevitably made.

The alternative approach introduced in this paper is to initially compute an extremely accurate solution which is nearly exact. The data base which results is extremely large. A controlled method of approximating this accurate solution is then pursued in an effort to compress the data base and increase the compatibility of the resulting data with the beam control system. Interestingly, the approach also makes excellent use of the fastest computation capabilities available on attached array processors. The method is fast, accurate, efficient and may ultimately be optimal.

II. THE IMAGE PROCESSING APPROACH

Kern[7] appears to have been the first to recognize the similarity between the proximity correction problem and the edge enhancement methods used in pattern recognition theory.[8] Essentially, the distortions imposed by the proximity effect amount to a loss of high spatial frequency content. Sharp edges and corners become rounded. Also, features which are enlarged or diminished during the development process can be regarded as resulting from incorrect or inconsistent developer threshold placement on a smeared effective dose profile which, in turn, can be modeled as a loss of high frequency edge definition. Kern observed that proximity corrections could be obtained by directly compensating the applied dose for the loss at high spatial frequencies in the resist in a manner which is analogous to classical methods in image processing.

For the purposes of this paper, we will limit our attention

to one-dimensional patterns. Extensions to two dimensions are straightforward. Essentially, the effective exposure, $E(x)$, in the resist is related to the applied dose $G(x)$ through a simple convolution:

$$E(x) = \int_{-\infty}^{\infty} G(x')F(x'-x)dx', \tag{1}$$

where $F(x)$ is the point-spread function resulting from an infinitesimally narrow beam, with that $G(x) = \delta(x)$. This equation is completely analogous to various models of distortions of images (resulting from finite aperture limitations in optics, for example). Equation (1) can be regarded as a Fredholm integral equation for $G(x)$ given a desired $E(x)$. However, if we permit the limits of integration to be infinite, then the integral equation has a well known solution which can be obtained by the Fourier transformation of Eq. (1):

$$e(j\omega) = g(j\omega)\cdot f(j\omega), \tag{2}$$

where e, g, and f are Fourier transforms for E, G, and F, respectively. Evidently, if we have a desired dose $D(x)$ and its Fourier transform is $d(j\omega)$, then a choice of $g(j\omega)$ given by

$$g_c(j\omega) = d(j\omega)/f(j\omega), \tag{3}$$

will lead to a compensated exposure $e_c(j\omega)$:

$$e_c(j\omega) = [d(j\omega)/f(j\omega)]\cdot f(j\omega) = d(j\omega). \tag{4}$$

The applied dose in Eq. (3) is termed Fourier precompensated.

The solution obtained by forming the Fourier inverse of Eq. (3), $G_c(x)$, is the *exact* solution for Eq. (1). Another major advantage of this approach is that the solution involves only operations which can be implemented on fast special purpose computing hardware. Conceivably, even faster hardware to perform these calculations may be built, as almost *any* degree of parallelism is possible for the Fast Fourier transform algorithm.[9]

The Fourier Precompensation method is not without its own peculiar set of deficiencies, however. The most serious difficulty is that it tends to produce compensated applied doses $G_c(x)$ which take on negative values at some locations, and such values cannot be physically realized. The second problem is that the $G_c(x)$ contains too much detail resulting from rapid oscillations. This tends to enlarge the data base undesirably. Nevertheless, the overwhelming computational superiority of this approach suggests that it offers a good starting point. The next three sections address these two deficiencies.

III. CONTROLLING THE NEGATIVE APPLIED DOSE

The negative values observed in the oscillating Fourier precompensated applied dose are a Gibbs phenomenon resulting from the sharp spatial transitions usually included in an ideal desired dose. Two features conspire to accentuate this Gibbs oscillation: the abrupt vertical rise and fall of the dose function, and the abrupt cessation of this vertical transition at the upper and lower desired dose values which causes sharp corners on the function. Kern[7] proposed modifying the desired dose by tilting the vertical transition and beveling the sharp corners with straight line segments at a still larger tilt angle. This greatly attenuates the negative dose values, but does not eliminate them. He then proposed clipping all remaining negative excursions of the applied dose at zero. For some point spread functions, this will prove adequate.

We have found that rounding the corners of the desired dose rather than beveling them tends to produce even smaller negative excursions in the ideal applied dose. Various *ad hoc* corner rounding fillets have been tried. Splines[10] offer some attractive possibilities in designing optimal corner rounding fillets. Literally any template which controls the negative excursion sufficiently, while preserving the vertical walls of the net effective dose, can be considered. However, we have not found clipping the negative applied dose to be satisfactory in all cases. Instead, we have found that adding a constant to the applied dose sufficient to guarantee its positive value is a useful alternative, when used with caution. Addition of a constant would tend to adversely affect the "on" time of the electron beam. Some form of combined offset and clipping can reduce this. However, simply reducing the applied dose to zero in certain areas which are relatively unoccupied by features can also have the same effect.

This will be discussed further with the examples in Sec. VI.

IV. WALSH TRANSFORM THINNING ALGORITHM

The voluminous detail presented by the Fourier precompensated dose must be reduced to keep the data base manageable and to keep the e-beam control data transfer efficient. This may be accomplished by an approximation process which attempts to reduce this detail while preventing the deterioration of the effective dose. One attribute of the approximate dose which improves its match to the e-beam system is that it should have the appearance of a step function. The dose remains constant spatially on one of the steps. At the very least this reduces the rate with which control information must flow to the e-beam. However, for variable shape spot machines (such as the IBM EL-2) the aperture can be set to exploit the size of any step.

Orthogonal expansions exist which employ step functions for their basis set. These are generally termed Walsh functions although distinct sets exist such as the Haar functions.[11] For the Walsh function two arguments are specified, the sequency number n and the space variable x (regarded as a normalized fraction of the maximum length, L). Discrete Walsh functions of size $N = 2^P$ can be defined in terms of bit representations of n and x:

$$\begin{aligned}\mathrm{WAL}(n{:}x) &= \mathrm{WAL}(n_{P-1},n_{P-2},\ldots,n_0;\, x_{P-1},x_{P-2},\ldots,x_0)\\ &= \prod_{r=0}^{P-1}(-1)^{n_{P-1-r}(x_r+x_{r+1})}.\end{aligned} \tag{5}$$

The functions are orthogonal, such that

$$\sum_{x=0}^{N-1}\mathrm{WAL}(m,x)\mathrm{WAL}(n,x) = N\delta_{m,n}, \tag{6}$$

and the Walsh transform of a function such as the definition dose $G(x)$ defined on a set of points x is given by

$$g_q = \frac{1}{N}\sum_{x=0}^{N-1} G(x)\mathrm{WAL}(q,x), \tag{7}$$

where the inverse can be shown to be

$$G(x) = \sum_{q=0}^{N-1} g_q \mathrm{WAL}(q,x), \tag{8}$$

(i.e., the Walsh transform is identical to its inverse except for the scale factor N).

One of the significant properties of the Walsh transform is Parseval's relation:

$$\frac{1}{N}\sum_{x=0}^{N-1}[G(x)]^2 = \sum_{q=0}^{N-1} g_q^2. \tag{9}$$

This is especially useful to us since the mean square error produced by deleting all the Walsh coefficients for $q > M-1$ in obtaining an approximation $G_A(x)$ to $G(x)$ can be determined from

$$G(x) - G_A(x) = \sum_{q=M}^{N-1} g_q \mathrm{WAL}(q,x), \tag{10}$$

which with the use of Eq. (9) leads to

$$\sum_{x=0}^{N-1}[G(x) - G_A(x)]^2 = N\sum_{q=M}^{N-1} g_q^2. \tag{11}$$

Hence, we can control the error (in the mean square sense) in approximating the generator dose resulting from deleting $g_M,\cdots,g_{N-1}$ by simply summing the squares of these Walsh coefficients. While the mean square error is not as precise a measure as the point-wise maximum error, it is still very useful.

One means for data base compression, therefore, is directly perceived when the data is stored in the form of its Walsh coefficients. Note that the remaining Walsh coefficients which are retained need not be further adjusted as they are already optimal in the mean square sense. That is, any other value for any of the coefficients other than that produced using Eq. (7) can only make the mean square error bigger.

V. IMPACT ON THE EFFECTIVE DOSE

The approximation process just described produces a compaction of the data base, but at a cost of a deviation of the precompensated dose G_c away from the correct answer. We must establish the impact that this error in the applied precompensated dose has on the net effective exposure E in the electron resist. We define $E_A(x)$ as the effective exposure resulting from the approximate precompensated dose, G_A, produced by the Walsh[12] thinning process.

In this section, we will switch from the discrete notation of the previous section to the continuous space variable x on $[0,L]$ since we are interested in the effective dose behavior everywhere on the resist. In this case,

$$G(x) = \sum_{q=0}^{N-1} g_q \mathrm{WAL}(q,x/L), \tag{12}$$

where x is viewed as continuous, and $\mathrm{WAL}(q,x/L)$ is zero outside of $[0,L]$. We equivalently form a discrete space of very high dimensions.

Now the effective dose satisfies Eq. 1. Hence, the mean square error in the effective dose resulting from thinning is:

$$\overline{\epsilon^2} = \frac{1}{L}\int_0^L |E(x) - E_A(x)|^2 dx$$
$$= \frac{1}{L}\int_0^L \left|\int_{-\infty}^{\infty}[G(x') - G_A(x')]f(x'-x)dx'\right|^2 dx. \tag{13}$$

From Eq. (10) we can write the following:

$$\overline{\epsilon^2} = \frac{1}{L}\int_0^L |h(x)|^2 dx, \tag{14}$$

where

$$h(x) = \sum_{q=M}^{N-1} g_q \int_{-\infty}^{\infty} \mathrm{WAL}(q,x'/L)f(x'-x)dx'. \tag{15}$$

Now $h(x)$ has a Fourier transform on $[-\infty,\infty]$ given by

$$H(j\omega) = \int_{-\infty}^{\infty} h(x)\exp(-j\omega x)\,dx$$
$$= \sum_{q=M}^{N-1} g_q \Xi(q,j\omega)\cdot F(j\omega), \tag{16}$$

where

$$\Xi(q,j\omega) = \int_{-\infty}^{\infty} \mathrm{WAL}(q,x/L)\exp(-j\omega x)dx, \tag{17}$$

and

$$F(j\omega) = \int_{-\infty}^{\infty} F(x)\exp(-j\omega x)dx. \tag{18}$$

By Parseval's Theorem

$$\int_{-\infty}^{\infty} h(x)^2 dx = \frac{1}{2\pi}\int_{-\infty}^{\infty} |H(j\omega)|^2 d\omega. \tag{19}$$

Now, note that $h(x)$ is nearly zero outside $[0,L]$. Only a small spillage occurs outside of this range due to the convolution with the point spread function in Eq. (15). Hence, we can make the integral limits in Eq. (14) infinite with only a small increase in its size

$$\overline{\epsilon^2} \leqslant \frac{1}{2\pi L}\int_{-\infty}^{\infty} |H(j\omega)|^2 d\omega$$
$$= \frac{1}{2\pi L}\int_{-\infty}^{\infty} |F(j\omega)|^2 \cdot \left|\sum_{q=M}^{N-1} g_q \Xi(q,j\omega)\right|^2 d\omega$$
$$\leqslant \frac{1}{2\pi L}\int_{-\infty}^{\infty} |F(j\omega)|^2 \left(\sum_{q=M}^{N-1} |g_q||\Xi(q,j\omega)|\right)^2 d\omega, \tag{20}$$

where we have used the inequality $|x+y| \leqslant |x| + |y|$. Also, by the same inequality we have the following bound using Eq. (17):

$$|\Xi(q,j\omega)| = \left|\int_0^L \mathrm{WAL}(q,x/L)\exp(-j\omega x)\,dx\right|$$
$$\leqslant \int_0^L |\mathrm{WAL}(q,x/L)|\,|\exp(j\omega x)|dx$$
$$= L, \tag{21}$$

since both the Walsh and complex exponential functions are bounded in $[0,L]$ by unity in magnitude. Hence,

$$\overline{\epsilon^2} \leqslant \frac{1}{2\pi}\int_{-\infty}^{\infty} |F(j\omega)|^2 d\omega \cdot \left(\sum_{q=M}^{N-1} |g_q|\right)^2. \tag{22}$$

Since the first integral is just the energy in the point spread function we can choose to normalize the mean square error by dividing by this factor defining

$$\overline{\epsilon_N^2} \leqslant \left(\sum_{q=M}^{N-1} |g_q|\right)^2. \tag{23}$$

Using the Cauchy–Schwarz inequality this may be further simplified to

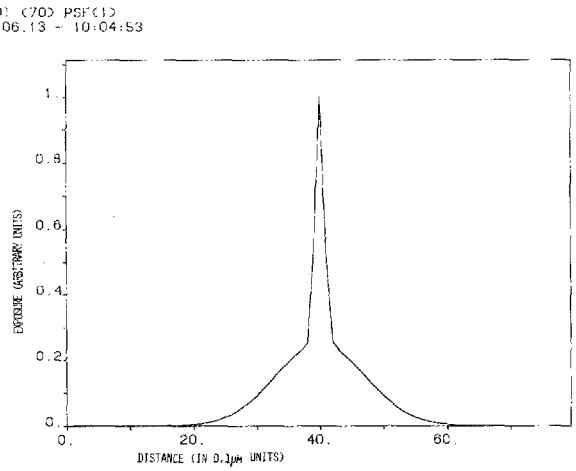

FIG. 1. Point spread function

$$F(x) = C_1 \cdot \exp[-(x^2/\beta_f^2)] + C_2 \cdot \exp[-(x^2/\beta_b^2)]$$

0.1 μm scale on x-axis. (Note: In all figures the y-axis is normalized.)

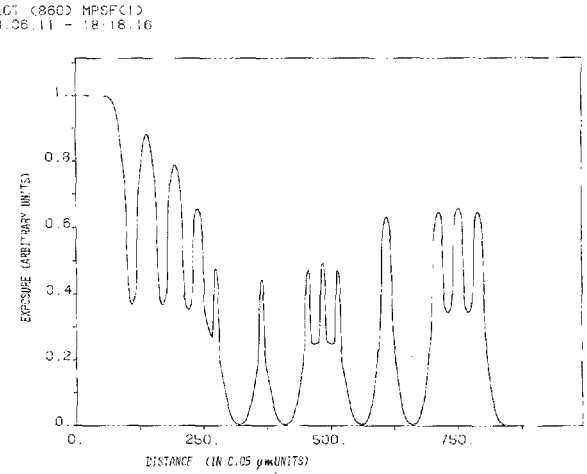

FIG. 3. Effective exposure absorbed by resist given ideal applied dose in Fig. 2.

$$\overline{\epsilon_N^2} \leqslant (N - 1 - M) \sum_{q=M}^{N-1} g_q^2, \tag{24}$$

which shows that the error bound on the resist is a scaled version of the mean square error in the generator function $G(x)$. However, the bound in Eq. (23) is tighter than that of Eq. (24) and is therefore preferable. Tighter bounds than this can be written, but they are not as easy to compute. Using Eq. (23) then the error in the effective dose or exposure can be monitored as Walsh coefficients are deleted. When the error bound becomes too large an excursion of the approximated exposure $E_A(x)$ may cross through the region where the developer threshold is placed causing drop-out or erroneous features to appear. At this point it becomes necessary to simulate the convolution Eq. (1) using the FFT as in Eq. (2). This gives the detailed point-to-point deviation from the correct answer rather than just the mean square error, but the computation is obviously much greater than that which is required to simply evaluate the bound in Eq. (23).

VI. COMPUTED RESULTS

In this study we have arbitrarily adopted the point spread function measured by Chang[1] for 0.6 μ thick PMMA on a silicon substrate with a beam acceleration voltage of 25 keV. For this case the double Gaussian form applies:

$$F(x) = C_1 \exp(-x^2/\beta_f^2) + C_2 \exp(-x^2/\beta_b^2), \tag{25}$$

where the first term is due to forward electron scattering in the resist and the second is due to backscattered electrons from the substrate. This is plotted in Fig. 1.

Figure 2 shows a conventional dose for a typical one-dimensional mask which consists of bars of various widths and spacings. In this figure as in all others the desired dose is normalized to unity. Left uncorrected, the effective exposure $E(x)$ is shown in Fig. 3.

The problems which arise when using this effective dose or exposure include: (a) the failure of the effective dose to rise and fall to uniform peak levels; (b) the rounding of the sharp edges of the desired dose which creates different sized fea-

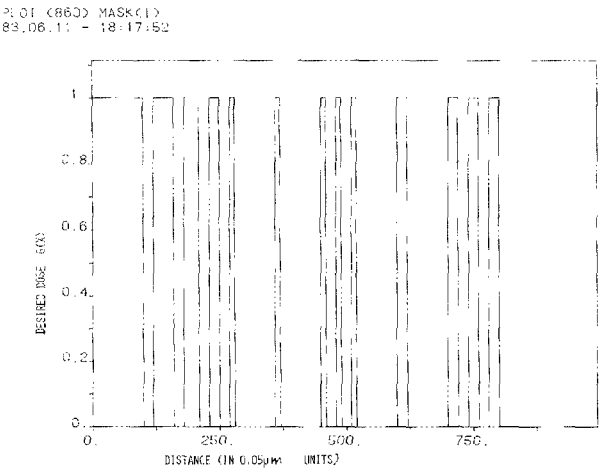

FIG. 2. Ideal applied dose, 0.05 μm x-axis scale. A 5.0 μm bar adjacent to a series of 2.0, 1.5, 1.0, and 0.5 μm bars separated by 1.0 μm gaps. An isolated 0.5 μm bar is next with 4.0 μm gaps followed by a trio of 0.5 μm bars with 1.0 μm gaps. This is repeated for 1.0 μm bars on the right.

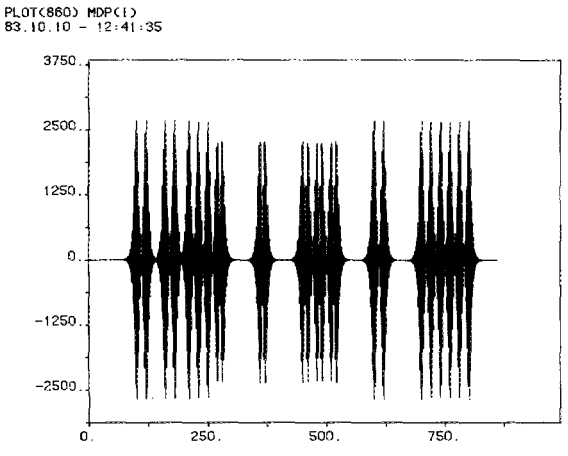

FIG. 4. Fourier precompensated dose given desired dose in Fig. 2.

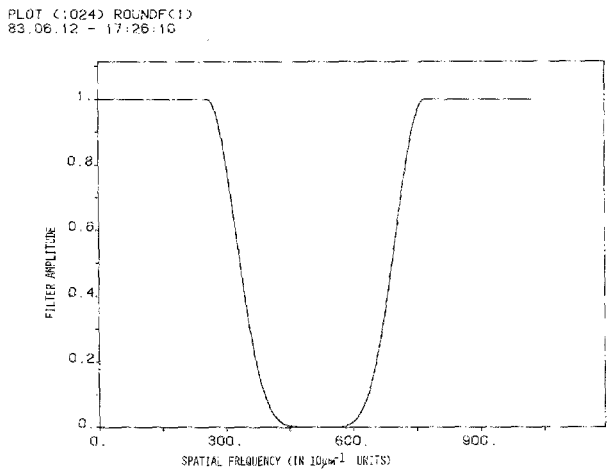

FIG. 5. Multiplicative function in frequency domain to reduce high frequency content. (Highest spatial frequency in center.)

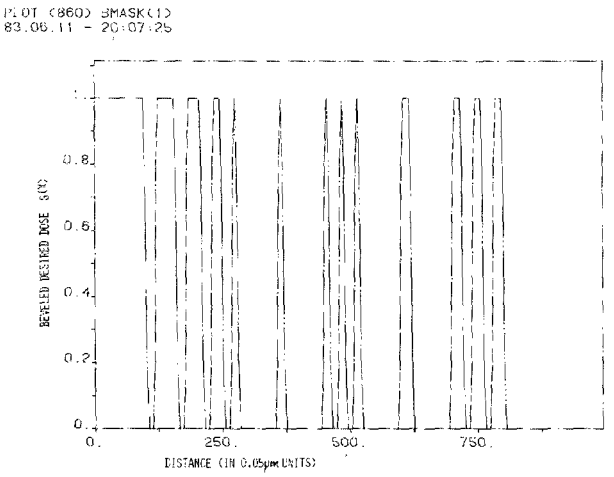

FIG. 8. Bevel model for desired effective dose (Ref. 7).

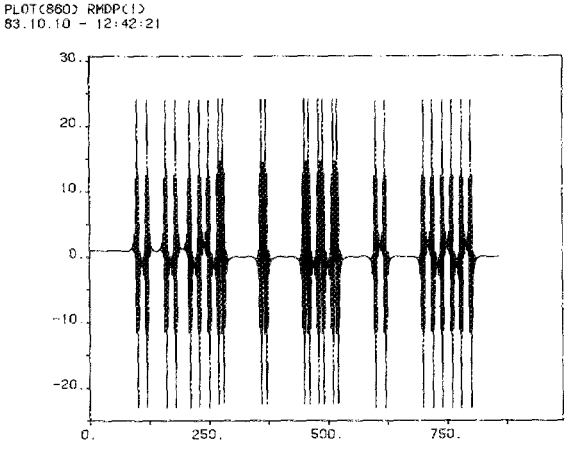

FIG. 6. Multiplicative function applied to Fig. 4. Figure still has a lot of high frequency content.

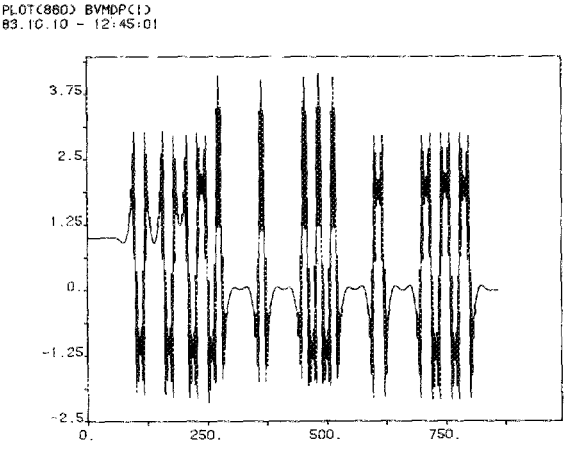

FIG. 9. Precompensated dose of Fig. 8. Figure still has a fair amount of high frequency components to be useful to the applied dose offsetted to zero.

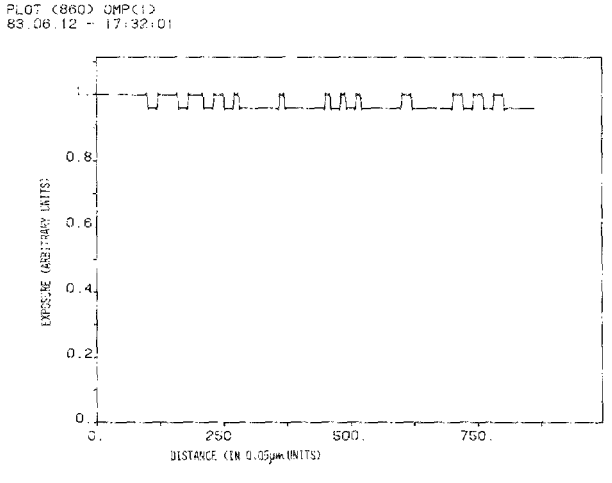

FIG. 7. Applying the dose of function in Fig. 6. The effective exposure is shown here, margin is too narrow for proper development.

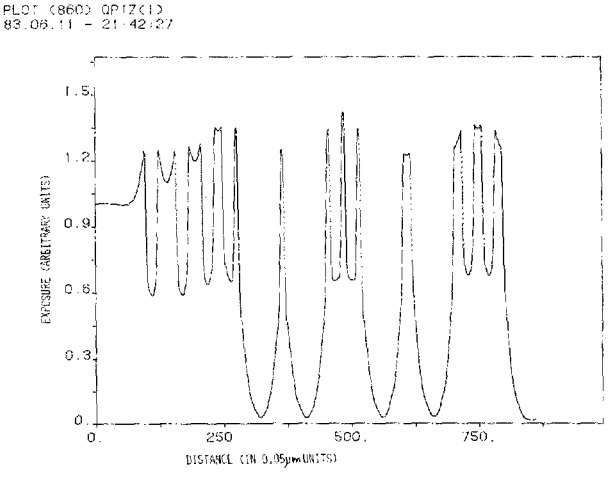

FIG. 10. Resultant effective exposure seen by resist with negative applied doses in Fig. 9 truncated to zero (Ref. 7).

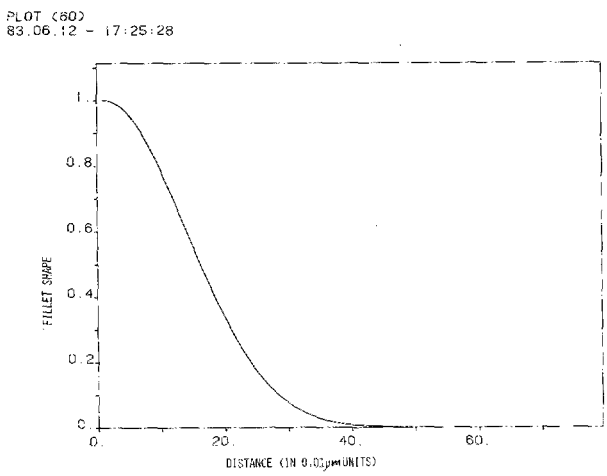

FIG. 11. A fillet used to model the desired effective dose. Note decreasing slope. 0.01 μm scale on x-axis.

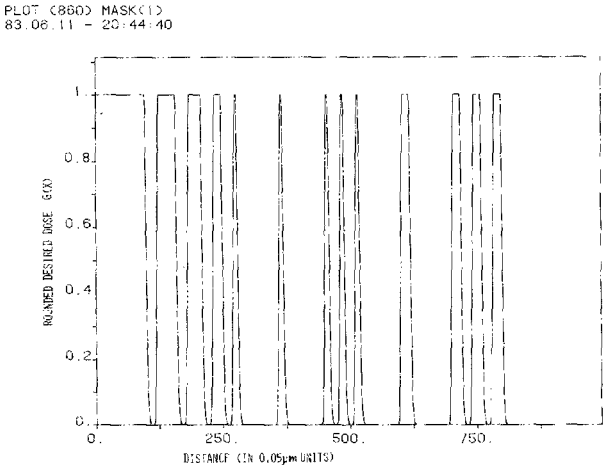

FIG. 12. Fillet model applied to ideal applied dose in Fig. 2.

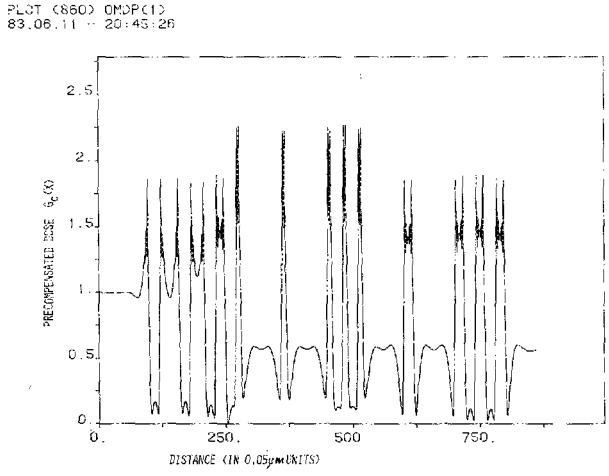

FIG. 13. Fourier precompensated applied dose for function in Fig. 12. (Includes additive offset to insure positive dose.)

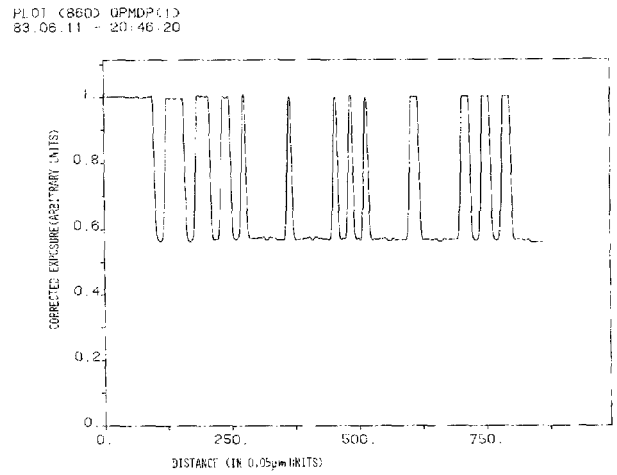

FIG. 14. Resultant effective exposure using fillet model.

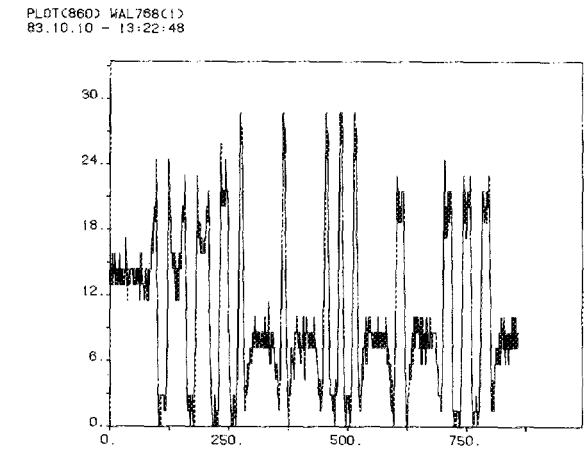

FIG. 15. Applied dose after 75% Walsh thinning process on dose in Fig. 13.

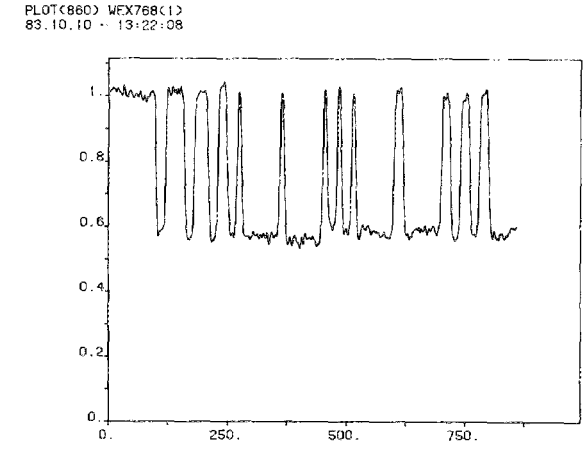

FIG. 16. Effective exposure of applied dose in Fig. 15. Pattern fidelity is still retained after a 3/4 reduction in data base.

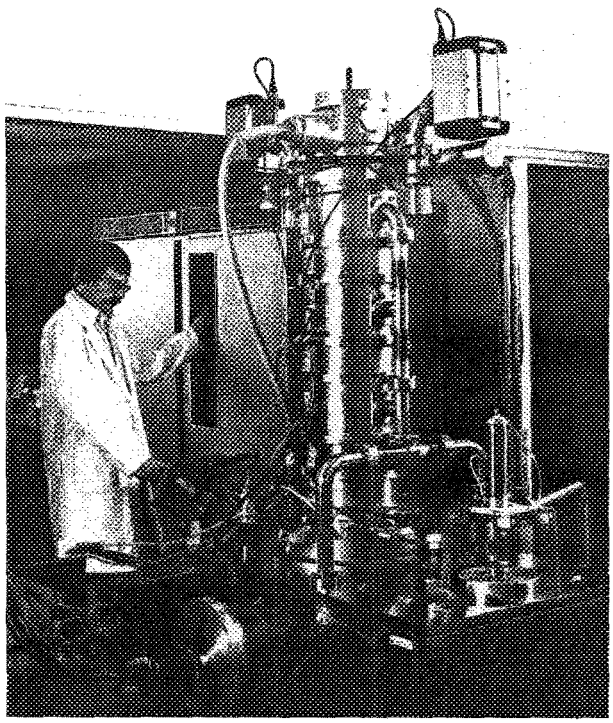

FIG. 17. IBM EL-2 direct-write electron beam lithography system. (Located at the Rensselaer Center for Integrated Electronics.)

tures depending on the developer threshold. By varying this threshold some features with effective dose below the threshold will not develop at all, while some which are above the threshold will begin to merge and eventually disappear altogether.

Fourier precompensation of the unrounded desired dose produces the applied dose in Fig. 4. This oscillates with very large (three orders of magnitude larger than the desired dose) amplitude excursions near the vertical transitions of the original desired dose. Clipping the negative dose for this oscillation produces unacceptable results as does the addition of a constant because the constant would have to be too large thereby masking the features completely.

One can attempt to minimize these oscillations by reattenuating some of the high frequency components which the precompensation process has amplified. Figure 5 shows a multiplicative window in the frequency domain with a high frequency roll-off tapered to minimize spatial oscillations using techniques of digital filter design.[9] The resulting applied dose appears in Fig. 6. Its relative magnitude has been reduced to the same range as the original desired dose. Adding a constant offset sufficient to guarantee a non-negative dose produces the resulting effective dose of Fig. 7.

To further control the negative dose excursions a bevel suggested by Kern[7] is introduced onto the desired dose as shown in Fig. 8, producing the applied dose in Fig. 9. Convolving with the point spread function gives the effective dose of Fig. 10. There is some corner rounding present and the threshold range containing missing features is a problem.

If instead of a bevel, a corner rounding fillet is employed at each step in the desired dose such as shown in Fig. 11, then the desired dose is shown in Fig. 12, the applied dose becomes Fig. 13. With offset addition the resulting net effective exposure becomes that of Fig. 14.

To simplify the data base a Walsh thinning process (which removed 75% of the coefficients) followed by quantization produces the applied dose shown in Fig. 15, and its effective exposure in Fig. 16. The degree of success achieved by the Walsh thinning process in reducing the data base (in the transform domain) is strongly dependent on the minimum feature size sought and the width and shape of the point spread function. In this case the minimum feature size is 0.5 μ while the point spread function contains a backscatter component several μm in width.

The Walsh transforms set probably does not represent the ultimate image processing transformation. Other transform function sets, specifically the Haar, are known to produce more powerful compressions, and these remain to be examined.

VII. EXPERIMENTAL RESULTS

A series of experiments have been recently initiated to verify this approach to proximity correction. The experiments employ the IBM EL-2 electron beam lithography tool (Fig. 17) at Rensselaer's Center for Integrated Electronics which operates at a beam voltage and current of 25 keV and 2 μA, respectively. Typically, 1 μm-thick films of IBM Terpolymer and PMMA resists were used. The vehicle used for proximity correction experiments, shown in Fig. 18, consisted of two pairs of rectangles separated by a space. The right pair received an uncorrected dose, while the left pair was

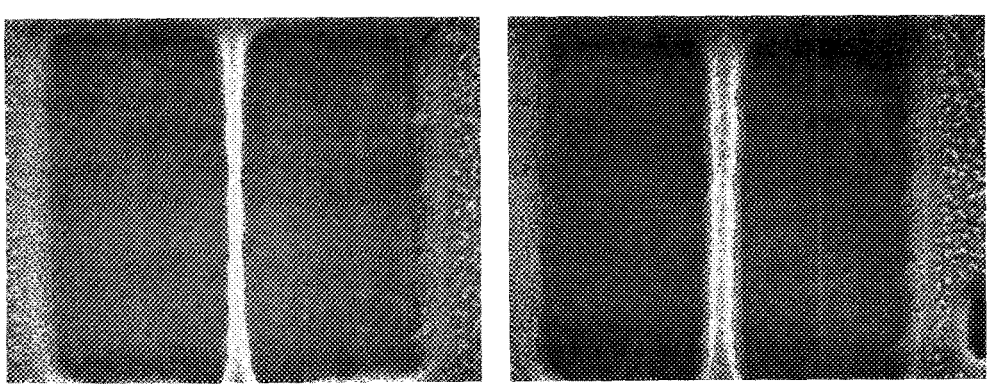

FIG. 18. Proximity correction using Walsh transform for pattern in terpolymer electron resist. Magnification is 1.1×10^4. The bar on the left is proximity effect corrected. The bar on right is uncorrected.

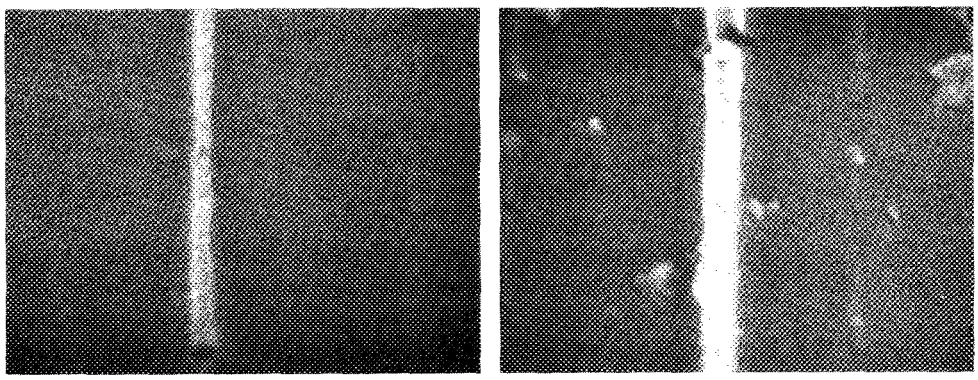

FIG. 19. Proximity correction using Walsh transform for pattern in PMMA electron resist. Magnification is 1.1×10^4. Proximity effect corrected bar and uncorrected bar on left and right, respectively.

corrected as discussed herein. Varied doses for correction were achieved by rewriting portions of the pattern utilizing the variable spot shaping and variable dose capabilities of the EL-2. In some cases, large effective doses were obtained by repeated exposure of a given area to small electron doses.

The initial experiments concentrated on obtaining more vertical resist properties from the corrected exposure levels. Figure 18 shows a SEM photograph (11 000×) of an uncorrected Terpolymer pattern. The bar separating the two rectangles exhibits a nonuniform profile with a "skirt" evident at the bottom of the bar. The bar in the left hand pattern has been obtained with a compensated dose which removed the skirt by increasing the dose at the edge of the pattern. The normal width of both bars is 0.4 μm, but the skirt effectively doubles the width of the uncorrected bar. A similar effect is observed in PMMA as shown in Fig. 19.

VIII. CONCLUSIONS

A dose adjustment technique for proximity correction has been examined which exploits a combination of Fourier precompensation (as suggested by Kern) corner rounding to minimize negative dose excursions, offset addition to cancel the remaining negative excursions, and Walsh transform "thinning" to compress the data base.

Criteria for estimating the effective dose error resulting from Walsh transform thinning have been discussed. Effects of dose quantization were simulated, and results of experiments using the IBM EL-2 were presented.

The conclusions of this study are: (a) the new approach appears computationally advantageous; (b) the data base can be made efficient.

ACKNOWLEDGMENTS

The authors wish to express their gratitude to IBM, especially the East Fishkill division, both for their donation of the EL-2 system to the Center for Integrated Electronics (CIE) and for their constant assistance, encouragement, and support. The authors also acknowledge recent financial support from the Semiconductor Research Cooperative, Dr. B. Agusta, research monitor, under agreement number 83-01-041. Finally, the authors wish to express their gratitude to other colleagues at the CIE for their assistance in this project, especially Mr. Mark Bourgeois.

[1]T. H. P. Chang, J. Vac. Sci. Technol. **12**, 1271 (1975).
[2]R. J. Hawryluk, J. Vac. Sci. Technol. **19**, 1 (1981).
[3]L. Karapipiris, I. Adesida, C. A. Lee, and E. D. Wolf, J. Vac. Sci. Technol. **19**, 1259 (1981).
[4]H. Sewell, J. Vac. Sci. Technol. **15**, 927 (1978).
[5]M. Parikh, J. Appl. Phys. **50**, 4371 (1979).
[6]E. Kratschmer, J. Vac. Sci. Technol. **19**, 1264 (1981).
[7]D. Kern, *9th International Conference on Electron and Ion Beam Science and Technology*, edited by R. Bakish (Electrochemical Society, Princeton, 1980), p. 326.
[8]H. C. Andrews *Computer Techniques in Image Processing* (Academic, New York, 1970).
[9]L. R. Rabiner and B. Gold, *Theory and Application of Digital Signal Processing* (Prentice–Hall, Englewood Cliffs, New Jersey, 1975).
[10]M. H. Schultz, *Spline Analysis* (Prentice-Hall, Engelwood Cliffs, New Jersey, 1973).
[11]D. F. Elliot and K. R. Rao, *Fast Transforms, Algorithms, Analysis, Applications* (Academic, New York, 1982).
[12]K. G. Beauchamp, *Walsh Functions and Their Applications* (Academic, New York, 1975).